DELPHI Collaboration

DELPHI 2001-071 CONF 499
10 June, 2001

Search for Charged Higgs Bosons in e+e- Collisions at LEP

M. Battaglia[1], M. Ellert[2], T. Ekelof[2], G. Gómez-Ceballos[3], A. Kiiskinen[4], P. Lutz[5] and F. Matorras[3]

[1]CERN, Geneva, Switzerland
[2]Uppsala University, Uppsala, Sweden
[3]Universidad de Cantabria, Santander, Spain
[4]Helsinki Institute of Physics, Helsinki, Finland
[5]CEA, Saclay, France

Abstract

A search for pair-produced charged Higgs bosons was performed in the data collected by the DELPHI detector at the high energy runs of LEP. Charged Higgs boson decays into tau leptons or c and s quarks were considered. No excess of data compared to the expected Standard Model processes was observed and a lower mass limit for charged Higgs bosons is set. Results are also presented as upper limits for the charged Higgs boson pair production cross-section.

Contributed Paper for EPS HEP 2001 (Budapest) and LP01 (Rome)

1 Introduction

The existence of a charged Higgs boson doublet is predicted by several extensions of the Standard Model. Pair-production of charged Higgs bosons occurs mainly via s-channel exchange of a photon or a Z^0 boson. In two-doublet models, the couplings are completely specified in terms of the electric charge and the weak mixing angle, θ_W, and therefore the production cross-section depends only on the charged Higgs boson mass. Higgs bosons decay predominantly to the heaviest fermions kinematically allowed, which in the case of charged Higgs bosons at LEP energies can be either a $\tau\nu_\tau$ pair or a cs quark pair. In order to ensure that the results are model independent, analyses of the three possible final states, $\tau\nu\tau\nu$, $c\bar{s}\bar{c}s$ and $c\bar{s}\tau\nu$, have been performed and described in this paper. The decay branching fraction to leptons and quarks has been treated as a free parameter in the combination of the results of these three analyses.

A search for pair-produced charged Higgs bosons was performed based on the data collected by DELPHI during the LEP runs at centre-of-mass energies from 189 GeV to 208 GeV.

A new technique was developed to improve the discrimination against the hadronic W decays in the search for $H^\pm$ candidates. Improved methods using the τ polarisation and boson production angles in the leptonic and semileptonic channels were used for rejection of W^+W^- background.

2 Data Analysis

Data collected during the years 1998, 1999 and 2000 at centre-of-mass energies from 189 GeV to 208 GeV were used. The integrated luminosities of the analysed data samples are summarised in Table 4. The DELPHI detector and its performance have already been described in detail elsewhere [1, 2].

Signal samples were simulated using the HZHA generator [3]. The background estimates from the different Standard Model processes were based on the following event generators: PYTHIA [4] for $q\bar{q}(\gamma)$, KORALZ [5] for $\mu^+\mu^-$ and $\tau^+\tau^-$, BABAMC [6] for e^+e^- and EXCALIBUR [7] for four-fermion final states. Two-photon interactions were generated with TWOGAM [8] for hadronic final states, BDK [9] for electron final states and BDKRC [9] for other leptonic final states.

Standard DELPHI criteria were used for particle quality cuts and are described in detail in [10].

In all three analyses the final background rejection was performed by using a likelihood technique. For each of the N discriminating variables, the fractions $F_i^{HH}(x_i)$ and $F_i^{bkg}(x_i)$ of respectively H^+H^- and background events, corresponding to a given value x_i of the i^{th} variable, were extracted from samples of simulated H^+H^- and background events normalised to equal size. The signal likelihood was computed as the normalised product of these individual fractions, $\prod_{i=1,N} F_i^{HH}(x_i)/(\prod_{i=1,N} F_i^{HH}(x_i) + \prod_{i=1,N} F_i^{bkg}(x_i))$.

2.1 The leptonic channel

The signature for $H^+H^- \to \tau^+\nu_\tau\tau^-\bar{\nu}_\tau$ is large missing energy and momentum and two acollinear and acoplanar jets containing either a lepton or one or a few hadrons. Tight requirements for good running of the most important sub-detectors were used in this

analysis in order to ensure good quality of the tracks. This results in slightly smaller integrated luminosities than in the hadronic channel (see Table 4).

2.1.1 Event preselection

To select leptonic events a total charged particle multiplicity between 2 and 6 was required. All particles in the event were clustered into jets using the LUCLUS algorithm [4] (d_{join} = 6.5 GeV/c^2) and only events with two reconstructed jets were retained. Both jets had to contain at least one charged particle and at least one jet had to contain not more than one charged particle. The angle between the two jets was required to be larger than 30°.

Two-fermion and two-photon events were rejected by requiring an acoplanarity larger than 13° if both jets were in the barrel region (43° $< \theta <$ 137°) and larger than 25° otherwise.

The two-photon background was further reduced by different energy requirements: the sum of the jet energies transverse to the beam direction, $E_\perp$, was required to be larger than $0.08\sqrt{s}$ if both jets were in the barrel region and larger than $0.1\sqrt{s}$ in other cases; the total transverse momentum, $p_\perp$, to be greater than $0.04\sqrt{s}$; the total energy detected within 30° around the beam axis to be less than $0.1\sqrt{s}$; and the total energy outside this region to be greater than $0.1\sqrt{s}$.

Additional τ identification cuts were applied to reject WW events were the W's have not decayed to $\tau\nu$. If the τ jet was identified as an electron it had to have a momentum below $0.13\sqrt{s}$ and an electromagnetic energy below $0.14\sqrt{s}$. For muons the momentum had to be below $0.13\sqrt{s}$. If a τ decay candidate particle was not identified as either a muon or an electron, it was considered to be a hadron and accepted as a τ decay particle without further requirements. Events in which the invariant mass of either of the jets was more than 3 GeV/c^2 were rejected.

The effects of the $\tau^+\nu_\tau\tau^-\bar{\nu}_\tau$ selection cuts are shown in Table 1 for the combined 189–208 GeV sample.

2.1.2 Final background discrimination

After these selections most of the remaining background consists of $\mathrm{W^+W^-} \to \tau^+\nu_\tau\tau^-\bar{\nu}_\tau$ events. Events from both the $\mathrm{H^+H^-}$ signal and the $\mathrm{W^+W^-}$ background have similar topologies and due to the presence of missing neutrinos in the decay of each of the bosons, it is not possible to reconstruct the boson mass. There are two important differences, however, that were used in order to discriminate the signal from the $\mathrm{W^+W^-}$ background: the boson polar angle and the τ polarisation.

Assuming that the ν_τ has a definite helicity, the polarisation of tau leptons originating from heavy boson decays is determined entirely by the properties of weak interactions and the nature of the parent boson. The helicity configuration for the signal is $\mathrm{H^-} \to \tau^-_R\bar{\nu}_{\tau R}$ ($\mathrm{H^+} \to \tau^+_L\nu_{\tau L}$) and for the $\mathrm{W^\pm}$ boson background it is $\mathrm{W^-} \to \tau^-_L\bar{\nu}_{\tau R}$ ($\mathrm{W^+} \to \tau^+_R\nu_{\tau L}$) resulting in $P_\tau^{\mathrm{H}} = +1$ and $P_\tau^{\mathrm{W}} = -1$. The angular and momentum distributions depend on polarisation and it is possible to build estimators of the τ polarisation to discriminate between the two contributions.

The τ decays were classified into the following categories: e, μ, π, $\pi + n\gamma$, 3π and others. The information on the τ polarisation was extracted from the observed kinematic distributions of the τ decay products, e.g. their angles and momenta. These estimators

are equivalent to those used at LEP I [11]. For charged Higgs boson masses close to the threshold, the boost of the bosons is relatively small and the τ energies are similar to those of the τ's from Z^0 decays (40–50 GeV).

A likelihood to separate the signal from the W^+W^- background was built using four 'independent' variables: the estimators of the τ polarisation and the polar angle of the decay products of both τ's. The distribution of that likelihood for data, expected backgrounds and 75 GeV/c^2 charged Higgs boson is shown in Fig 1.

cut	data	total bkg.	4-fermion	other bkg.	ε_{75}
Leptonic selection	159861	161652.7	911.3	160741.4	71.9%
Acoplanarity cut	16789	16473.7	706.8	15766.9	60.2%
Energy cuts	532	553.7	528.5	25.2	45.3%
τ identification	64	63.7	57.7	6.0	33.9%

Table 1: The total number of events observed and expected backgrounds in the leptonic channel after the different cuts used in the analysis. The last column shows the efficiency for a charged Higgs boson signal with $m_{H^\pm} = 75$ GeV/c^2.

2.2 The hadronic channel

In the fully hadronic decay channel, each charged Higgs boson is expected to decay into a $c\bar{s}$ pair, producing a four-jet final state. The two sources of background in this channel are the $q\bar{q}gg$ QCD background and fully hadronic four-fermion final states. As the significance of the Z^0Z^0 pairs for the analysis is negligible compared to the W^+W^- pairs, the four-fermion sample is referred to as W^+W^- in the rest of the paper.

2.2.1 Event preselection

Events were clustered into four jets using the Durham algorithm [12]. The particle quality requirements and the first level hadronic four-jet event selection followed in this analysis were the same as for the DELPHI neutral Higgs analysis [13].

In order to reject more effectively three-jet like QCD background events the Durham clustering parameter $y_{4\to3}$ value for transition from four to three jets was required to be greater than 0.003. Events with a clear topology of more than four jets were rejected by adding a cut on the $y_{5\to4}$ value for transition from five to four jets at 0.010 because of their worse di-jet mass resolution after forcing them into four jets.

Energy-momentum conservation was imposed by performing a 4-C fit on these events and the difference between the two di-jet masses for each jet pairing was computed. A 5-C fit, assuming equal boson masses, was applied in order to improve the di-jet mass resolution. The di-jet combination giving the smallest 5-C fit χ^2 was selected for the mass reconstruction. Events for which the minimum of the 5-C fit χ^2 divided by the number of degrees of freedom exceeded 1.5 or the difference of the masses computed with the same pairing after the 4-C fit exceeded 15 GeV/c^2 were rejected.

2.2.2 Final background rejection

The largest contribution to the part of the selected sample of W^+W^- events whose reconstructed mass is below the W mass peak comes from picking one of the wrong di-jet pairings. These wrongly paired events are characterised by larger difference between the masses of the two di-jets, i.e. the two boson candidates. As the initial quark antiquark pairs are connected by a QCD colour field, in which the hadrons are produced in the fragmentation process, the wrongly paired events can also be identified using a method of colour connection reconstruction [14].

The colour connection reconstruction method is based on the fact that, in the rest frame of the correctly paired initial quark antiquark pair, the hadrons that are produced in this colour string should have small transverse momenta relative to the quark antiquark pair axis. This could be distorted by hard gluon emission but such events are suppressed with the $y_{5\to4}$ Durham parameter cut. When boosted into a rest frame of a wrongly paired quark pair the transverse momenta of the particles relative to the quark quark axis are larger. The correct pairing is found by calculating the sum of transverse particle momenta in each of the three possible pairing hypotheses. The pairing chosen using the colour connection reconstruction is compared to the pairing chosen using the minimisation of the χ^2 of the 5-C kinematical fit. The output of this comparison, called $p_\perp$-veto, is either agreement or disagreement and it is used later in the analysis as one of the variables in the background rejection likelihood.

The production polar angle of the positively charged boson discriminates between W^+W^- and Higgs pairs. This angle is reconstructed as the polar angle of the di-jet with the higher charge, where the jet charge is calculated as a momentum weighted sum of the charges of the particles in the jet [15]. The distribution of this variable allows the discrimination of the signal from the background of wrongly paired W^+W^- events and QCD events, even though in these latter cases the variable does not correspond to a true boson production angle.

Since the charged Higgs boson is expected to decay to $c\bar{s}$ in its hadronic decay mode, the QCD and W^+W^- backgrounds can be partially suppressed by selecting final states consistent with being $c\bar{s}\bar{c}s$. A flavour tagging algorithm has been developed for the study of multiparton final states [16]. This tagging is based on nine discriminating variables: three of them are related to the identified lepton and hadron content of the jet, two depend on kinematical variables and four on the reconstructed secondary decay structure. The finite c lifetime is exploited to distinguish between c and light quark jets, while the c mass and decay multiplicity are used to discriminate against b jets. Furthermore s and c jets can be distinguished from u and d jets by the presence of an identified energetic kaon. The responses for the individual jets are further combined into an event $c\bar{s}\bar{c}s$ probability.

The four variables described above: di-jet pair mass difference, di-jet momentum polar angle, event $c\bar{s}\bar{c}s$ probability and the $p_\perp$-veto, were combined to form an event anti-WW likelihood function separating W^+W^- events from H^+H^- events. The response of this likelihood also discriminates H^+H^- from the QCD background events.

An anti-QCD likelihood was formed using all four variables which were used in the anti-WW likelihood and, in addition, two variables which can be used to separate QCD background from pair-produced bosons: the clustering algorithm parameter $y_{4\to3}$ and the event acoplanarity.

The effects of the different sets of cuts are shown in Table 2 for the combined 189–

208 GeV sample. The distribution of the anti-QCD likelihood on the preselection level and the distribution of the anti-WW likelihood after a cut on the anti-QCD likelihood are shown in Fig 2. The reconstructed mass distribution for data, expected backgrounds and signal after the anti-QCD and anti-WW cuts is shown in Fig 3.

cut	data	total bkg.	4-fermion	other bkg.	ε_{75}
4-jet presel.	6548	6394.0	4156.1	2237.9	85.2%
Durham y_{cut}	4883	4756.2	3485.7	1270.5	72.6%
5-C fit χ^2	3807	3809.6	2926.6	883.0	61.3%
Mass diff.	2753	2784.4	2270.6	513.8	51.0%
anti-QCD	1357	1388.5	1273.1	115.4	37.0%
anti-WW	1040	1058.5	956.5	102.0	33.9%

Table 2: The total number of events observed and expected backgrounds in the hadronic channel after the different cuts used in the analysis. The last column shows the efficiency for a charged Higgs boson signal with $m_{H^\pm} = 75$ GeV/c^2.

2.3 The semileptonic channel

In this channel one of the charged Higgs bosons decays into a $c\bar{s}$ quark pair, while the other decays into $\tau\nu_\tau$. Such an event is characterised by two hadronic jets, a τ candidate and missing energy carried by the neutrinos. The dominating background processes are QCD $q\bar{q}g$ event production and semileptonic decays of W^+W^-. The same requirements for good running of the most important sub-detectors were used as in the analysis of the leptonic channel.

2.3.1 Event preselection

At least 15 particles, of which at least 8 were charged, were required. The total energy of the observed particles had to exceed $0.30\sqrt{s}$. The missing transverse momentum had to be greater than $0.08\sqrt{s}$ and the modulus of the cosine of the angle between the missing momentum and the beam had to be less than 0.8. Events were also required to have no neutral particles with energy above 40 GeV.

After clustering into three jets using the Durham algorithm, the clustering parameter $y_{3\to2}$ was required to be greater than 0.003, and each jet had to contain at least one charged particle. The jet with the smallest charged particle multiplicity was treated as the τ candidate and if two or more of the jets had the same number of charged particles, the jet with smallest energy was chosen. The τ candidate was required to have no more than six particles, of which no more than three were charged.

2.3.2 Final background rejection

The mass of the decaying bosons was reconstructed using a constrained fit requiring energy and momentum conservation with the known beam energy and imposing the masses of the two bosons to be equal. The three components of the momentum vector of the ν_τ and the magnitude of the τ momentum were treated as free parameters, reducing the number

of degrees of freedom of the fit from 5 to 1. Only events with a reconstructed mass above 40 GeV/c^2 and a χ^2 below 2 were selected.

Separate likelihood functions were defined to distinguish the signal events from the QCD and the W^+W^- backgrounds, in a manner similar to that used for the other channels described above.

To define the anti-QCD likelihood, the acollinearity of the event, the polar angle of the missing momentum, the logarithm of the clustering parameter $y_{3\to2}$, and the product of the τ jet energy and the smaller of the two angles between the τ jet and one of the other jets were used as discriminating variables.

For the event anti-WW likelihood the variables used were the reconstructed polar angle of the negatively charged boson (where the charge was taken to be that of the leading charged particle of the τ jet), the angle between the boson and the τ in the boson rest frame, the energy of the τ jet, the classification of the decay of the τ candidate (e, μ, π, $\pi + n\gamma$, 3π and others), and the cs probability of the hadronic di-jet.

The effects of the different sets of cuts are shown in Table 3 for the combined 189–208 GeV sample. The distribution of the anti-QCD likelihood on the τ selection level and the distribution of the anti-WW likelihood after a cut on the anti-QCD likelihood are shown in Fig 4. The reconstructed mass distribution for data, expected backgrounds and signal after anti-QCD and anti-WW cuts is shown in Fig 5.

cut	data	total bkg.	4-fermion	other bkg.	ε_{75}
preselection	10284	9796.0	4844.8	4951.2	81.7%
τ selection	3361	3567.4	2817.2	750.2	58.6%
χ^2	2751	2819.7	2430.7	389.0	50.5%
likelihoods	498	498.2	366.1	32.1	34.0%

Table 3: The total number of events observed and expected backgrounds in the semi-leptonic channel after the different cuts used in the analysis. The last column shows the efficiency for a charged Higgs boson signal with $m_{H^\pm} = 75$ GeV/c^2.

3 Results

3.1 Selection efficiencies and uncertainties

The number of real data and background events and the estimated efficiencies for these selections for different $H^\pm$ masses are summarised in Table 4 for the three final states.

Uncertainties in the expected background and in the signal efficiency were accounted for. Small contributions to these uncertainties are due to uncertainties in the luminosity measurement and in the cross-section estimates of the generated Monte Carlo samples. The event selection and systematic errors in the leptonic analysis are very similar to those in the DELPHI leptonic W^+W^- analysis [17]. The largest part of the background and signal efficiency uncertainties in the leptonic channel is due to the limited simulation statistics available. Combining these uncertainties gives a total uncertainty of the order of 10% in the background rate and 5% in the signal efficiency. The largest contribution in the semileptonic and hadronic analyses is due to differences in the distributions of the

Chan.	$\sqrt{s}$	lum.	data	total bkg.	ε_{75}
$\tau\nu\tau\nu$	189	153.8	16	15.0± 1.5	34.2±1.6%
$\tau\nu\tau\nu$	192	24.5	3	2.8± 0.3	34.2±1.6%
$\tau\nu\tau\nu$	196	72.4	10	8.6± 0.8	34.2±1.6%
$\tau\nu\tau\nu$	200	81.8	8	9.0± 0.9	33.5±1.6%
$\tau\nu\tau\nu$	202	39.4	2	4.4± 0.4	33.5±1.6%
$\tau\nu\tau\nu$	205	145.2	18	16.8± 1.0	33.9±1.6%
$\tau\nu\tau\nu$	207	60.3	7	7.2± 0.6	33.1±1.6%
$cscs$	189	154.3	288	267.8±16.1	33.1±2.0%
$cscs$	192	25.5	36	42.7± 2.6	33.1±2.0%
$cscs$	196	77.1	141	130.0± 7.8	33.8±2.0%
$cscs$	200	83.9	133	138.8± 8.3	33.5±2.0%
$cscs$	202	40.8	55	68.6± 4.1	33.5±2.0%
$cscs$	205	164.5	295	305.1±16.1	34.9±2.1%
$cscs$	207	60.6	92	107.7± 5.7	34.6±2.1%
$cs\tau\nu$	189	153.8	154	141.4± 8.5	35.2±1.8%
$cs\tau\nu$	192	24.5	30	24.8± 2.2	38.2±2.3%
$cs\tau\nu$	196	72.4	89	71.8± 6.3	38.2±2.3%
$cs\tau\nu$	200	81.8	79	81.5± 7.2	38.2±2.3%
$cs\tau\nu$	202	39.4	35	38.9± 3.4	38.2±2.3%
$cs\tau\nu$	205	145.2	122	134.0±14.7	34.1±2.7%
$cs\tau\nu$	207	60.7	51	56.8± 6.9	34.6±2.7%

Table 4: Integrated luminosity, observed number of events, expected number of background events and signal efficiency for different decay channels and centre-of-mass energies (75 GeV/c^2 signal mass).

preselection and likelihood variables in data and simulation. The systematic error of the efficinecy of the common DELPHI hadronic four-jet preselection has been estimated to be ±4% [13]. The uncertainties of the other selection variables have been estimated by comparing the shapes of the variable distributions in data and simulation. This has been done at the preselection level where the background event rate is so large that a possible signal would have no effect on the global shapes of the variables. The agreement of all variables has been found to be satisfactory to the level of a few percent. Combining these errors, a total uncertainty of ±6% has been estimated for the background rate and signal efficiency in the hadronic channel. In the semileptonic channel the combined background error estimate is ±6–9% depending on the energy sample and the error of the signal efficiency is of the order of ±6%. The combined error estimates are also included in Table 4.

3.2 Determination of mass and cross-section limits

No significant signal like excess of events compared to the expected backgrounds was observed in any of the three final states investigated. A lower limit for a charged Higgs boson mass was derived at 95% confidence level as a function of the leptonic Higgs decay branching ratio BR(H $\rightarrow \tau\nu_\tau$). The confidence in the signal hypothesis, CL_s, was

calculated using a likelihood ratio technique [18].

The background and signal probability density functions of one or two discriminating variables in each channel were used. The data samples collected in seven different centre-of-mass energies were treated in the combination separately as individual experiments. In the hadronic and semileptonic channels the two discriminating variables were the reconstructed mass and the anti-WW likelihood while in the leptonic channel only one background discrimination likelihood was used since mass reconstruction is not possible. The distributions of the discriminating variable for signal events, obtained by the simulation at different $H^{\pm}$ mass values for each $\sqrt{s}$, were interpolated for intermediate mass values. To obtain the expected signal rate at any given mass the signal efficiencies were fitted with polynomial functions,

A Gaussian smearing of the central values of the number of expected background events by their estimated uncertainties was introduced in the limit derivation program.

The results are summarised in Fig 6. A lower $H^{\pm}$ mass limit of $M_{H^{\pm}} > 73.8$ GeV/c^2 can be set at the 95% confidence level, independently of the branching ratio BR($H \to \tau\nu_\tau$). The mean of the limits obtained from a large number of simulated Gedanken experiments is 73.8 GeV/c^2 and the median of the limits is 75.4 GeV/c^2.

The results are also expressed as 95% confidence level upper limits for the charged Higgs boson production cross-section as a function of the charged Higgs boson mass. These cross-section limits were determined for each mass point by scaling the expected 2HDM signal cross-section up or down untill the confidence level of exclusion reached 95%. Fig. 7–9 show the excluded cross-sections for BR($H \to \tau\nu_\tau$) = 1.0, BR($H \to \tau\nu_\tau$) = 0.0 and BR($H \to \tau\nu_\tau$) = 0.5. These excluded cross-sections are given for 207 GeV centre-of-mass energy.

4 Conclusion

A search for pair-produced charged Higgs bosons was performed using the full statistics collected by DELPHI at LEP at centre-of-mass energies from 189 GeV to 208 GeV analysing the $\tau\nu\tau\nu$, $c\bar{s}\bar{c}s$ and $c\bar{s}\tau\nu$ final states. No significant excess of candidates was observed and a lower limit on the charged Higgs mass of 73.8 GeV/c^2 is set at 95% confidence level. Results are also presented as upper limits for the charged Higgs boson pair production cross-section as a fuction of the charged Higgs boson mass.

Acknowledgements

We are greatly indebted to our technical collaborators, to the members of the CERN-SL Division for the excellent performance of the LEP collider, and to the funding agencies for their support in building and operating the DELPHI detector.
We acknowledge in particular the support of
Austrian Federal Ministry of Science and Traffics, GZ 616.364/2-III/2a/98,
FNRS–FWO, Belgium,
FINEP, CNPq, CAPES, FUJB and FAPERJ, Brazil,
Czech Ministry of Industry and Trade, GA CR 202/96/0450 and GA AVCR A1010521,
Danish Natural Research Council,
Commission of the European Communities (DG XII),

Direction des Sciences de la Matière, CEA, France,
Bundesministerium für Bildung, Wissenschaft, Forschung und Technologie, Germany,
General Secretariat for Research and Technology, Greece,
National Science Foundation (NWO) and Foundation for Research on Matter (FOM), The Netherlands,
Norwegian Research Council,
State Committee for Scientific Research, Poland, 2P03B06015, 2P03B1116 and SPUB/P03/178/98,
JNICT–Junta Nacional de Investigação Científica e Tecnológica, Portugal,
Vedecka grantova agentura MS SR, Slovakia, Nr. 95/5195/134,
Ministry of Science and Technology of the Republic of Slovenia,
CICYT, Spain, AEN96–1661 and AEN96-1681,
The Swedish Natural Science Research Council,
Particle Physics and Astronomy Research Council, UK,
Department of Energy, USA, DE–FG02–94ER40817.

References

[1] P. Aarnio *et al.* (DELPHI Collaboration), Nucl. Instr. and Meth. **A 303** (1991) 233.

[2] P. Abreu *et al.* (DELPHI Collaboration), Nucl. Instr. and Meth. **A 378** (1996) 57.

[3] P. Janot, in CERN report 96-01, Vol. 2, p. 309 (1996).

[4] T. Sjöstrand, Comp. Phys. Comm. **82** (1994) 74.

[5] KORALZ 4.0 generator: S. Jadach, B.F.L. Ward, Z. Was, Comp. Phys. Comm. **79** (1994) 503.

[6] F.A. Berends, R. Kleiss, W. Hollik, Nucl. Phys. **B 304** (1988) 712.

[7] F.A. Berends, R. Pittau, R. Kleiss, Comp. Phys. Comm. **85** (1995) 437.

[8] S. Nova, A. Olcheski and T. Todorov, in CERN Report 96-01, Vol. 2. p. 224.

[9] F.A. Berends, P.H. Daverveldt, R. Kleiss, Comp. Phys. Comm. **40** (1986) 271, 285 and 309.

[10] P. Abreu *et al.* (DELPHI Collaboration), E. Phys. J. **C 2** (1998) 581

[11] P. Abreu *et al.* (DELPHI Collaboration), Zeit. Phys. **C 67** (1995) 183.

[12] S. Catani *et al.* Phys. Lett. **B 269** (1991) 432.

[13] P. Abreu *et al.* (DELPHI Collaboration), E. Phys. J. **C 10** (1999) 563.

[14] A. Kiiskinen, V. Nomokonov and R. Orava, Using colour portraits in identifying the quark-antiquark pairs in heavy boson decays, DELPHI 98-91 CONF 159.

[15] P. Abreu *et al.* (DELPHI Collaboration), CERN EP 2001-006 (Accepted by Phys.Lett.B)

[16] A similar jet flavour tagging technique has been used in determination of $|V_{cs}|$ at LEP II: P. Abreu *et al.* (DELPHI Collaboration), Phys. Lett. **B 439** (1998) 209.

[17] P. Abreu *et al.* (DELPHI Collaboration), Phys. Lett. **B 479** (2000) 89.

[18] A.L. Read, in CERN report 2000-015, p. 81

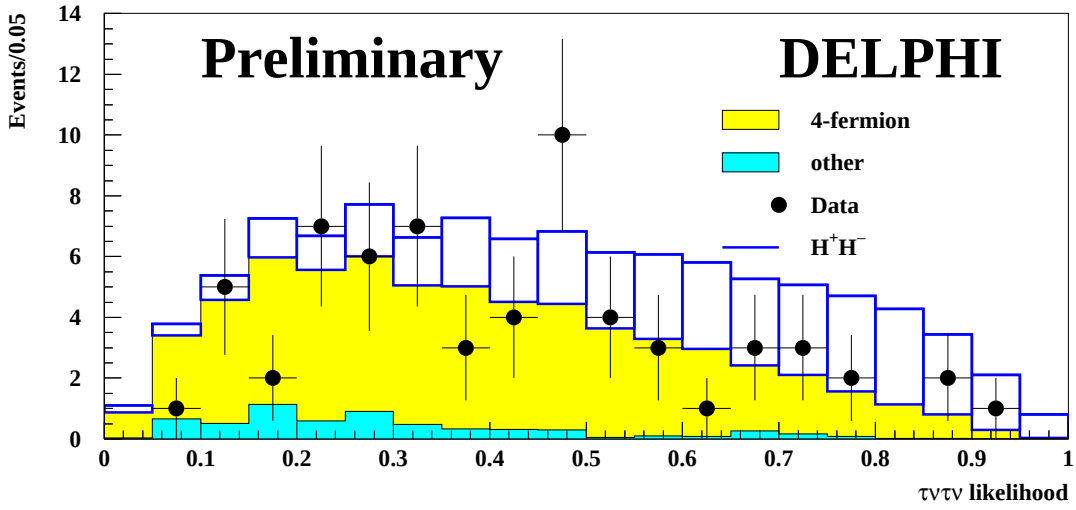

Figure 1: Distribution of the anti-WW likelihood for leptonic events at 189–208 GeV. The histogram for 75 GeV/c^2 charged Higgs boson signal has been normalised to the production cross-section and 100% leptonic branching ratio and added to the backgrounds.

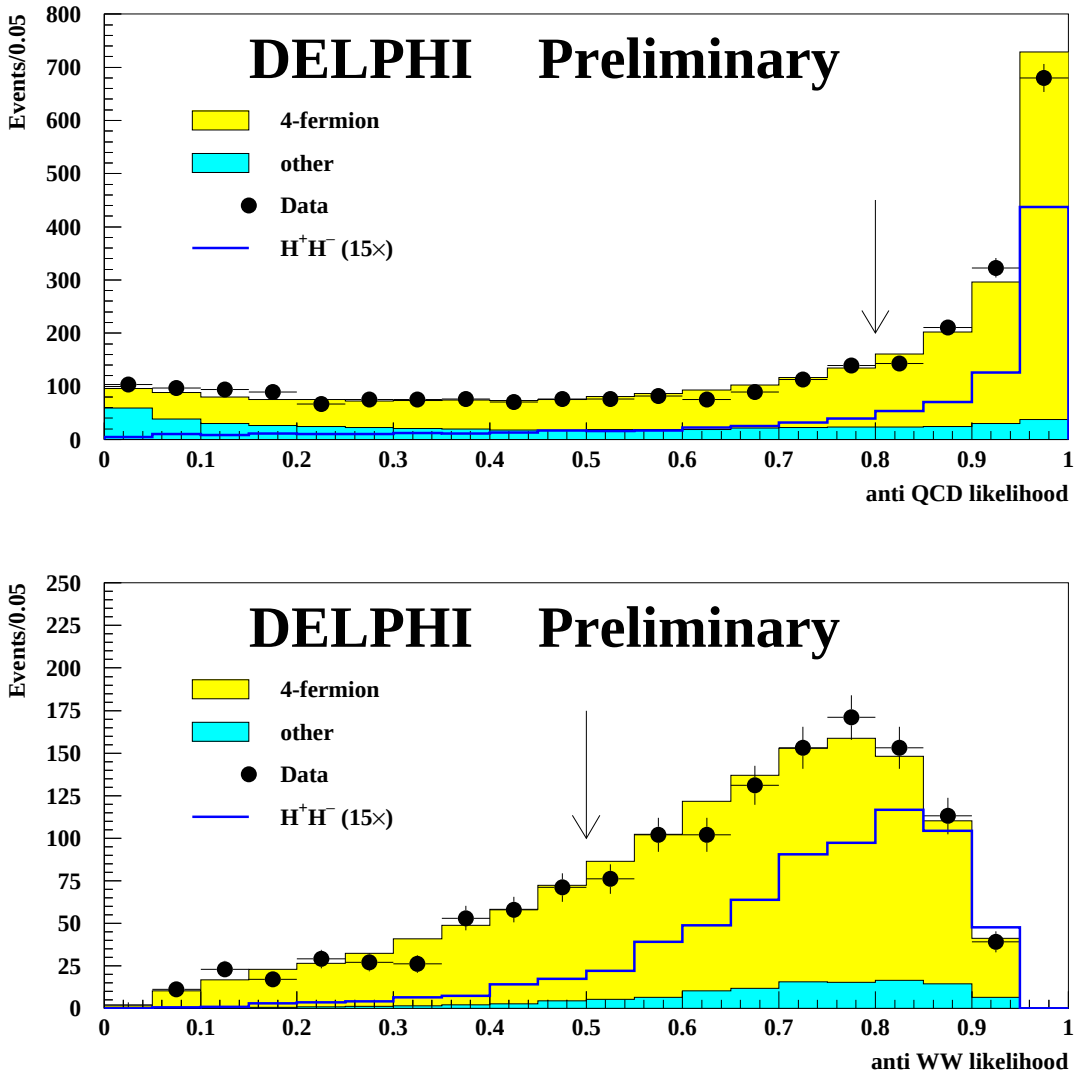

Figure 2: Distributions of the anti-QCD and anti-WW likelihoods for hadronic events at 189–208 GeV. The anti-QCD likelihood is plotted on the preselection level and the anti-WW likelihood after a cut on the anti-QCD likelihood. The generated H^+H^- signal mass is 75 GeV/c^2 and the signal histograms have been normalised to the production cross-section and 100% hadronic branching ratio, multiplied by a factor of 15 and superimposed on the background histograms. The arrows indicate the cut values, below which events were rejected.

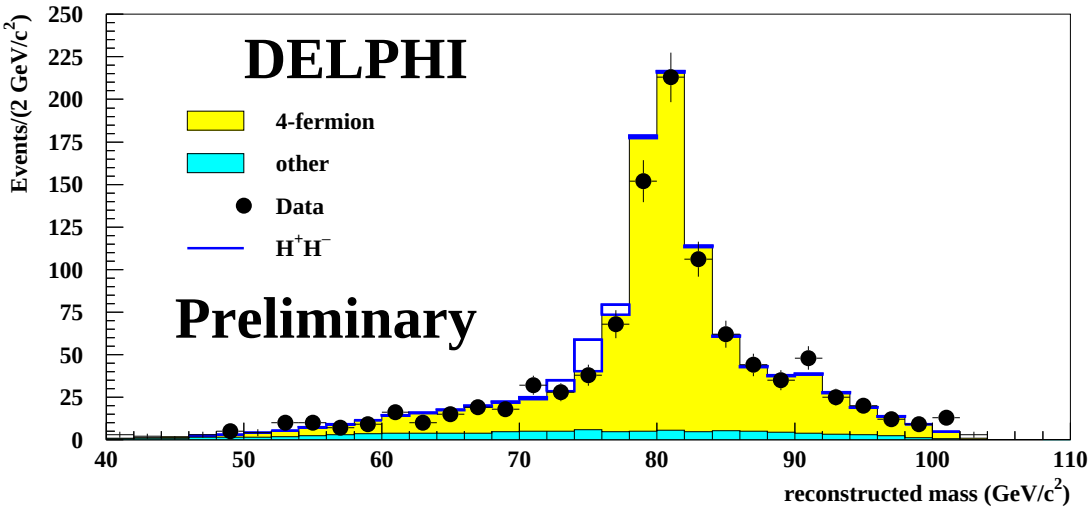

Figure 3: Reconstructed mass distribution of hadronic events at 189–208 GeV at the final selection level. The generated H^+H^- signal mass is 75 GeV/c^2 and the signal histograms have been normalised to the production cross-section and 100% hadronic branching ratio and added to the backgrounds.

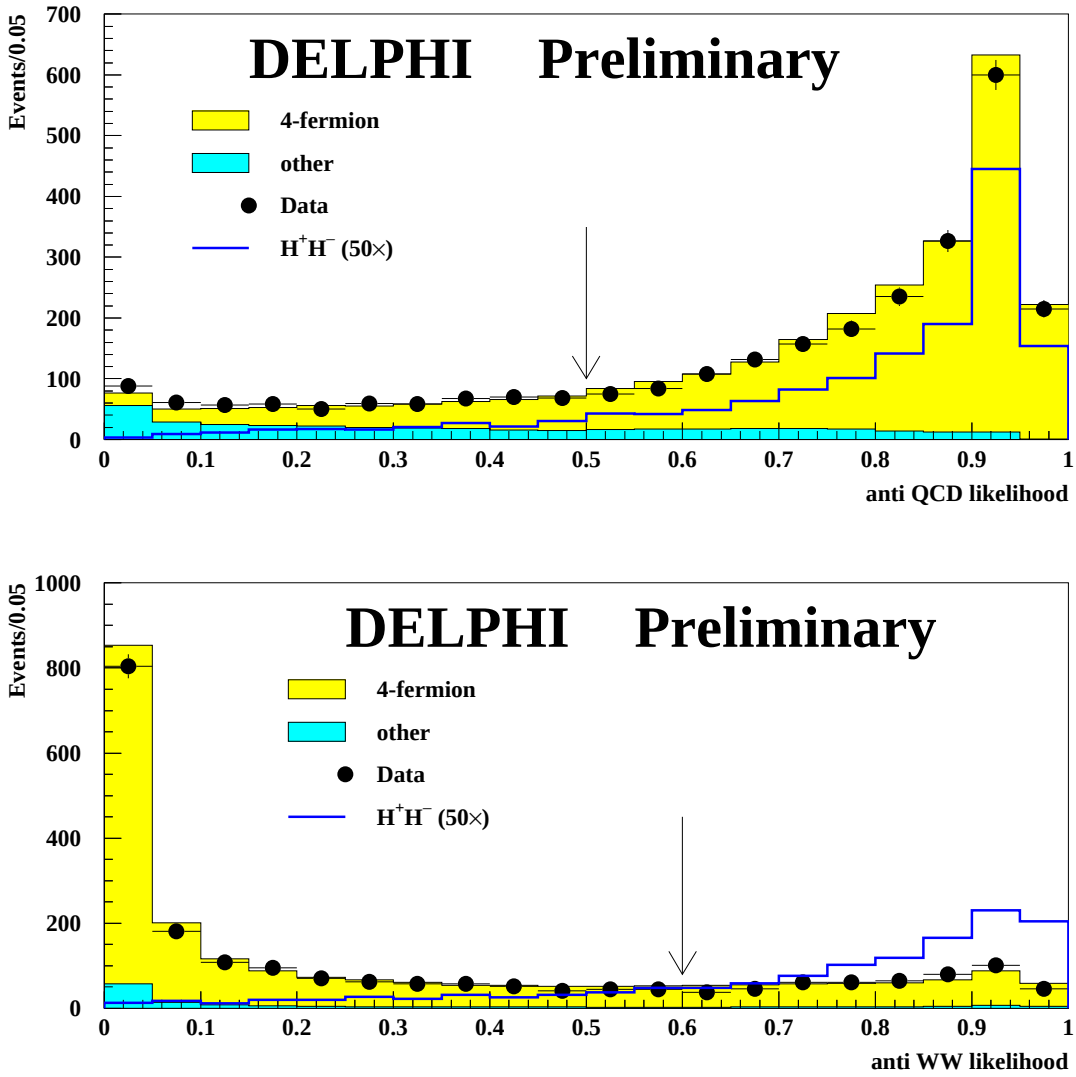

Figure 4: Distributions of the anti-QCD and anti-WW likelihoods for semileptonic events at 189–208 GeV. The anti-QCD likelihood is plotted on the preselection level and the anti-WW likelihood after a cut on the anti-QCD likelihood. The generated H^+H^- signal mass is 75 GeV/c^2 and the signal histograms have been normalised to the production cross-section and 50% leptonic branching ratio, multiplied by a factor of 50 and superimposed on the background histograms. The arrows indicate the cut values, below which events were rejected.

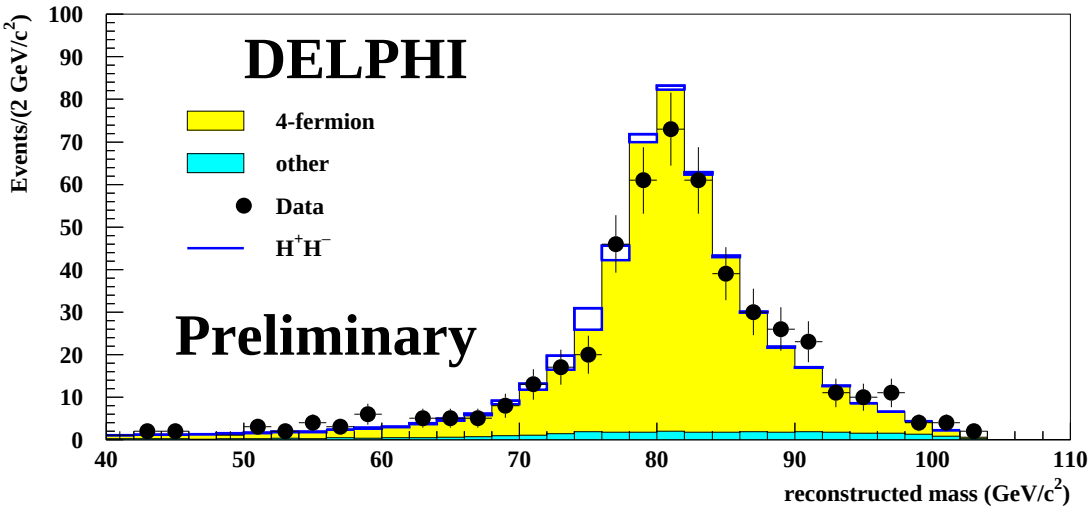

Figure 5: Reconstructed mass distribution of semileptonic events at 189–208 GeV at the final selection level. The generated H^+H^- signal mass is 75 GeV/c^2 and the signal histogram has been normalised to the production cross-section and 50% leptonic branching ratio and added to the backgrounds.

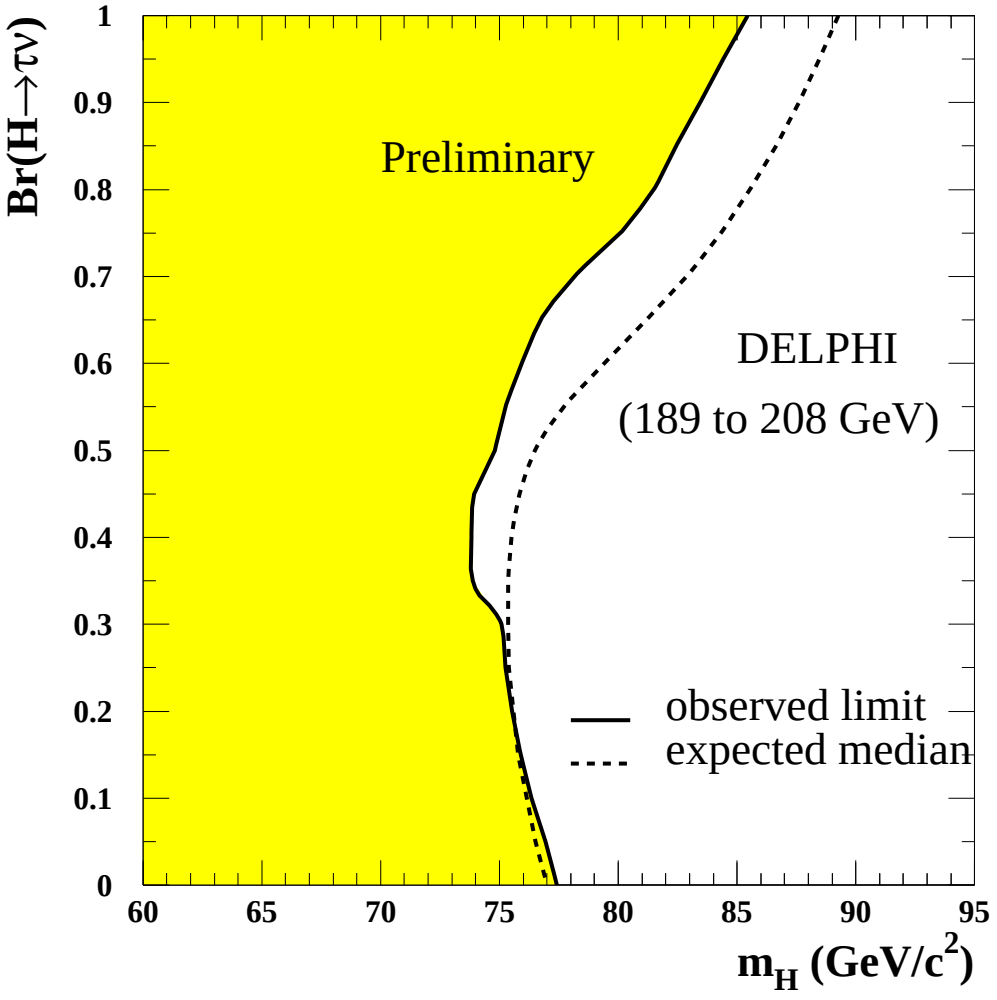

Figure 6: The 95% confidence level observed and expected exclusion regions for $H^{\pm}$ in the plane BR($H \rightarrow \tau\nu_\tau$) vs. $M_{H^{\pm}}$ obtained from a combination of the search results in the hadronic, semileptonic and fully leptonic decay channels at $\sqrt{s}$ = 189–208 GeV. The expected median is the value which has 50% of the values obtained in Gedanken experiments below and 50% above.

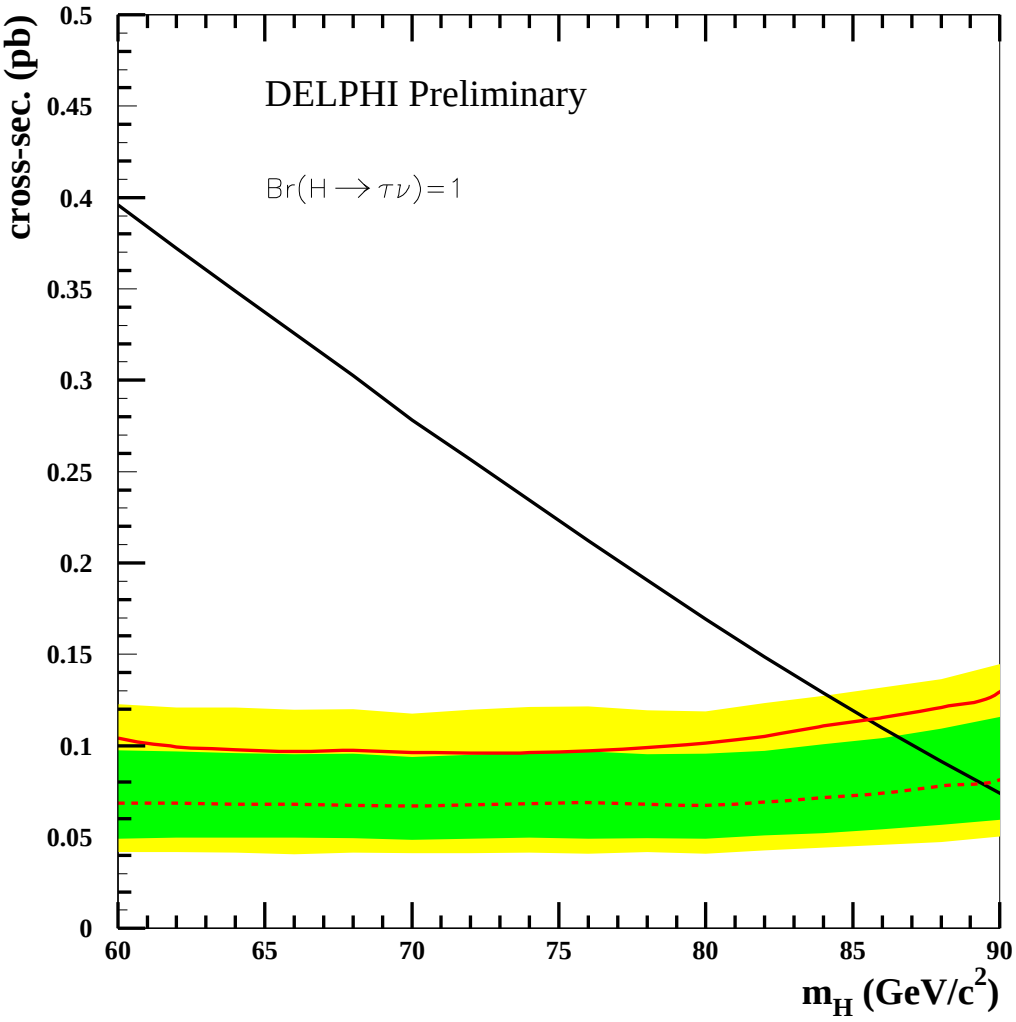

Figure 7: 95% confidence level upper limit for charged Higgs boson pair production with BR($H \rightarrow \tau\nu_\tau$) = 1.0 as a function of the charged Higgs boson mass. The dashed line shows the expected upper limit with one and two standard deviation bands and the solid line the observed upper limit of the cross-section. The solid black diagonal line shows the 2HDM prediction. Cross-sections are given for 207 GeV centre-of-mass energy.

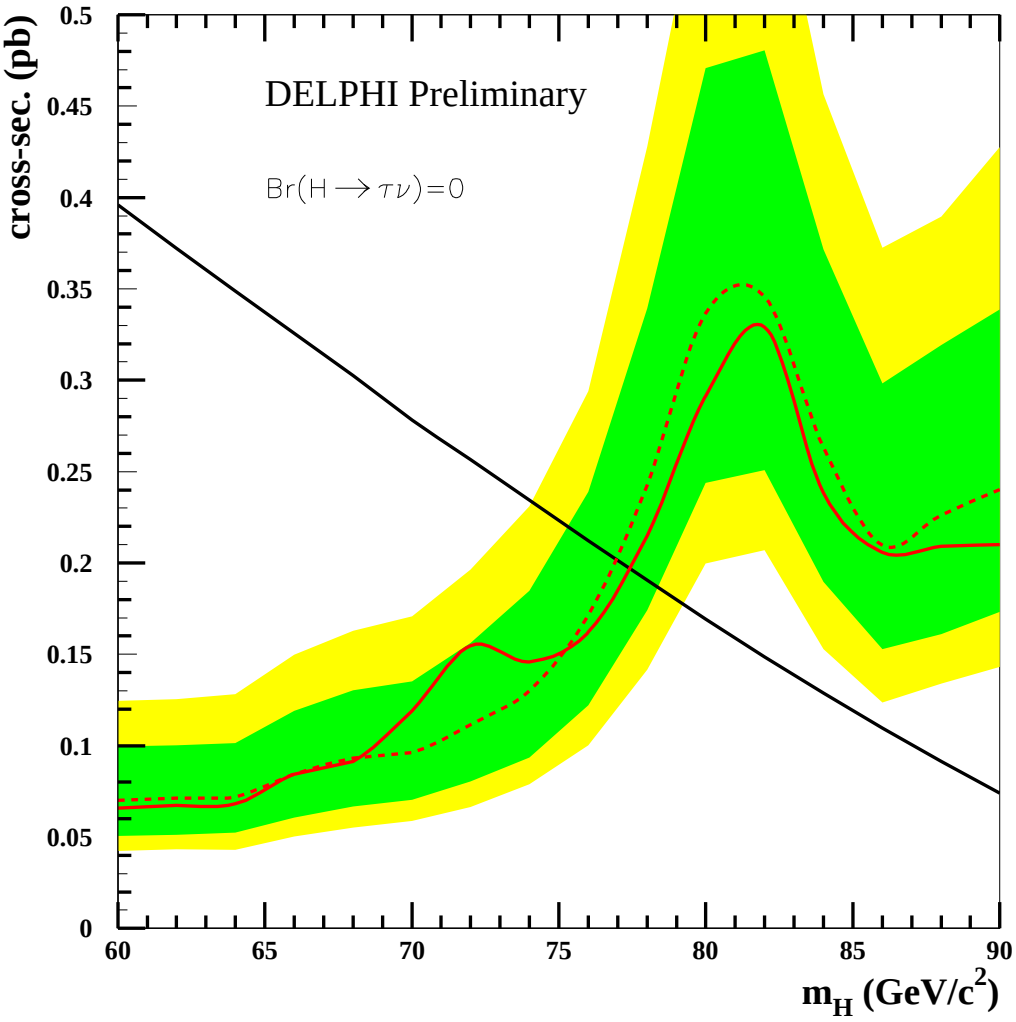

Figure 8: 95% confidence level upper limit for charged Higgs boson pair production with BR($H \rightarrow \tau\nu_\tau$) = 0.0 as a function of the charged Higgs boson mass. The dashed line shows the expected upper limit with one and two standard deviation bands and the solid line the observed upper limit of the cross-section. The solid black diagonal line shows the 2HDM prediction. Cross-sections are given for 207 GeV centre-of-mass energy.

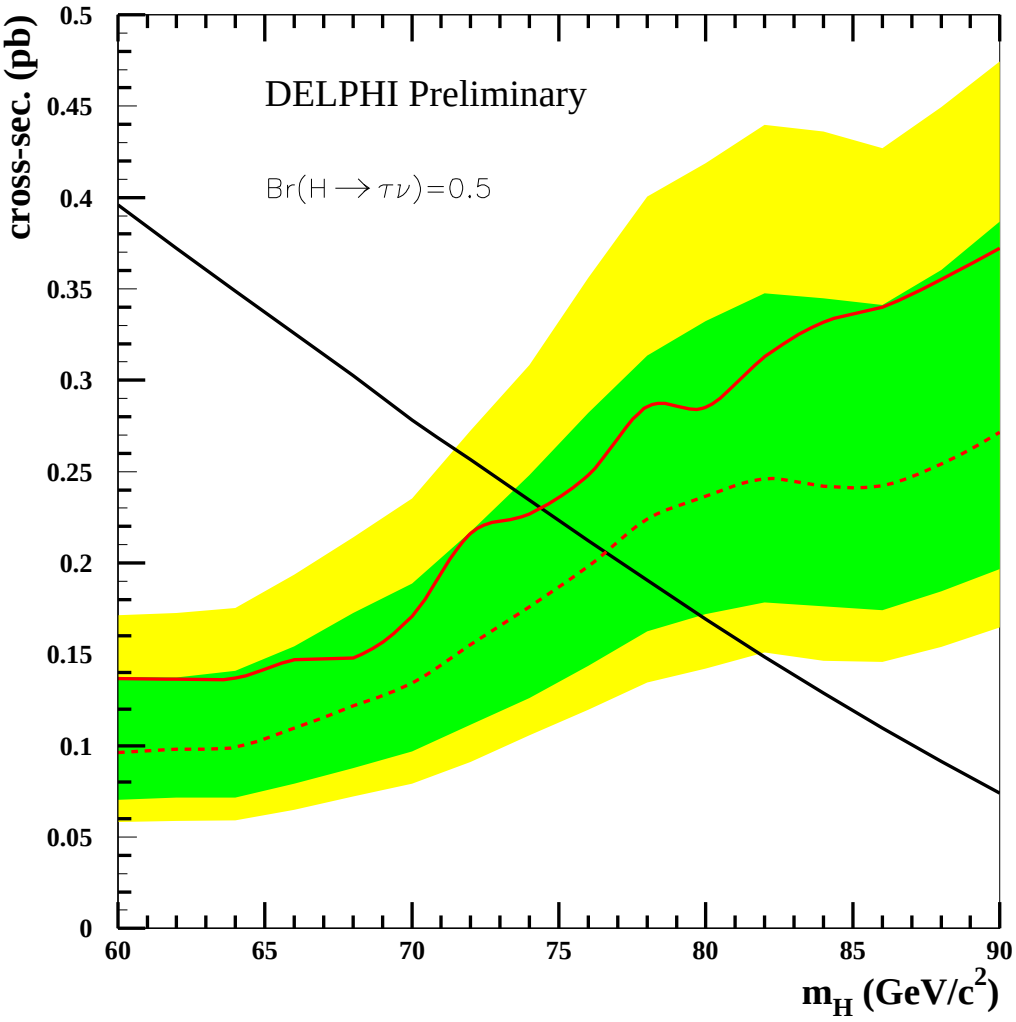

Figure 9: 95% confidence level upper limit for charged Higgs boson pair production with $\mathrm{BR}(H \to \tau\nu_\tau) = 0.5$ as a fuction of the charged Higgs boson mass. The dashed line shows the expected upper limit with one and two standard deviation bands and the solid line the observed upper limit of the cross-section. The solid black diagonal line shows the 2HDM prediction. Cross-sections are given for 207 GeV centre-of-mass energy.